Iranian Journal of Materials Forming 13 (4) (2026) 4-14

Online ISSN: 2383-0042

IJMF

Iranian Journal of Materials Forming

Journal Homepage: http://ijmf.shirazu.ac.ir

Research Article

Effect of Interpass Annealing on the Microstructure, Nanoindentation Hardness, and Electrical Conductivity of 20-µm Cold-Rolled Copper Foils

Amin Adel Shahbazi[1], Hamid Reza Shahverdi[1*] and Ali Akbar Mottahedi[2]

[1] Department of Materials Engineering, Tarbiat Modares University, Tehran, Iran
[2] Department of Advanced Materials and Renewable Energy, Iranian Research Organization for Science and Technology, Tehran, Iran

ARTICLE INFO

Article history:

Received: 9 December 2025
Reviewed: 15 April 2026
Revised: 28 April 2026
Accepted: 2 May 2026

Keywords:

Tough pitch copper
Printed circuit board
Recrystallization
Grain size
Foil rolling

Please cite this article as:

Shahbazi, A. A., Shahverdi, H. R., & Mottahedi, A. A. (2026). Effect of interpass annealing on the microstructure, nanoindentation hardness, and electrical conductivity of 20-µm cold-rolled copper foils. *Iranian Journal of Materials Forming*, *13*(4), 4-14. https://doi.org/10.22099/IJMF.2026.55041.1366

ABSTRACT

Copper foils play essential roles in electronic technologies, including lithium-ion batteries, printed circuit boards, and electrical interconnects, where microstructure, hardness, and electrical conductivity critically determine performance. Achieving the optimal combination of these properties is therefore central to producing high-quality foils. In this work, 20-µm-thick copper foil was fabricated from tough pitch copper (TPC) through cold rolling, and interpass annealing was applied to tailor and improve these key characteristics.

The material was first rolled from 100 µm to 30 µm, followed by interpass annealing for all samples except A0. Rolling was continued to achieve a final thickness of 20 µm. Annealing treatments were performed at 150, 200, 250, and 300 °C for 10, 15, 20, and 30 minutes. Microstructure, hardness, and electrical conductivity were characterized using optical microscopy, nanoindentation, and four-point probe measurements.

The as-rolled sample (A0) showed elongated, highly deformed grains (17.64 µm), elevated hardness (124.09 HV), and the lowest conductivity (84.39% IACS). Significant improvements were observed in samples B4 and C1, where recrystallization produced refined grains (4.01 µm in B4 and 3.47 µm in C1), reduced hardness (64.56 HV and 55.36 HV, respectively), and enhanced conductivity (88.99% and 89.76% IACS, respectively). Continued annealing led to grain growth, with D4 exhibiting the highest conductivity (96.29% IACS).

Overall, the influence of interpass annealing was evaluated across all processing conditions, and the results indicated that the routes used for samples B4 and C1 were optimal for producing 20-µm copper foil suitable for electronic applications. Depending on available equipment, either route can be selected for industrial production.

1. Introduction

Copper foil is a vital strategic material with extensive applications in printed circuit boards (PCBs), lithium-ion batteries, and the broader electronics industry. With the continued proliferation of electronic devices, electric vehicles, and clean energy technologies, the demand for high performance copper foil is steadily increasing [1]. Copper foil is primarily manufactured through

* Corresponding author
E-mail address: shahverdi@modares.ac.ir (H. R. Shahverdi)
https://doi.org/10.22099/IJMF.2026.55041.1366

electrodeposition or via a thermomechanical process involving rolling and annealing [1]. This research specifically focuses on rolled annealed (RA) copper foil.

The functional performance of copper foil is determined by its inherent properties. Consequently, the meticulous control and characterization of electrical, mechanical, and microstructural properties during the rolling and annealing process are crucial for ensuring the desired final performance of the copper foil [2].

Extensive research has been dedicated to the rolling and annealing of copper. However, a significant gap exists concerning the specific application of these processes to thin sections like foil. Moreover, many prior studies have focused on evaluating only one or two final properties of the copper foil, neglecting a comprehensive analysis that integrates key process parameters with the simultaneous investigation of critical material characteristics [3]. While previous investigations often adopted a purely academic viewpoint, this research prioritizes the establishment of an optimized process window. This defined parameter range is essential for achieving industry-standard properties and producing copper foil suitable for specific industrial applications. Furthermore, comprehensive studies examining the diverse properties of copper foil at a precise thickness of 20 µm are scarce [4]. This research gap is addressed herein by concurrently evaluating key properties such as electrical conductivity, hardness, and microstructure. The synergistic effects of these properties on overall performance and their optimization are thoroughly discussed [5].

Although established resources like the ASM Handbook: Copper and copper alloys offer broad insights into copper annealing, the unique characteristics of 20 µm copper foil, notably its high surface-to-volume ratio, demand a more refined examination of annealing parameters (temperature and time) within a meticulously defined operational range [1].

The primary objective of this research is to define an industrially applicable process window for the production of copper foil through rolling and annealing, targeting desirable final properties. A subsequent aim is the comprehensive and systematic investigation of the influence of interpass annealing parameters on the foil's electrical conductivity, hardness, and microstructure. The ultimate goal is to identify one or two optimal interpass annealing conditions that yield the best combination of these properties. Finally, the findings of this study are anticipated to be effective in producing 20 µm copper foil with electronic grade quality.

In this work, after several rolling passes and performing interpass annealing to reach a thickness of 20 µm, metallography and optical microscopy were used to investigate the microstructure, the four-point probe method was used to examine the electrical conductivity, and nanoindentation was used to measure the hardness.

2. Experimental Procedure

2.1. Material preparation

The initial material used in this study was a tough pitch copper sheet (TPC grade) with a thickness of 100 µm. The chemical composition was determined using optical emission spectrometry. The measured composition is shown in Table 1.

2.2. Cold rolling and interpass annealing process

The cold rolling process was carried out using a laboratory two-high rolling mill with a motor power of 5.5 kW, a roll diameter of 110 mm, and a rolling speed of 30 revolutions per minute. The as-received copper sheet (100 µm thick) was cold rolled to an intermediate thickness of 30 µm.

Interpass annealing was then performed at four different temperatures (150, 200, 250, and 300 °C) and four holding times (10, 15, 20, and 30 minutes) to study the effect of annealing parameters on the microstructure

Table 1. Chemical composition of the TPC sheet (wt.%)

Cu	Zn	P	S	Ni	Pb	Fe
99.9805	0.0091	0.035	0.0019	0.0008	0.0006	0.0005
Sb	**Al**	**Sn**	**As**	**Si**	**Se**	
0.0004	0.0004	0.0004	0.0003	0.0003	0.0002	

and properties of the foils. The annealing treatments were conducted in a tubular furnace under a protective atmosphere of mixed hydrogen and argon gases to prevent oxidation. After annealing, the samples were air-cooled to room temperature.

Following the interpass annealing step, the foils were again cold rolled to a final thickness of 20 µm. The annealed samples were coded according to their temperature-time conditions, as shown in Table 2.

2.3. Microstructural characterization

The surface microstructure of the copper foils was examined using an Olympus BX51 optical microscope manufactured by Olympus Corporation, Japan.

Before examination, the samples were prepared through grinding, polishing, and chemical etching using an etchant composed of 10 ml $FeCl_3$ + 30 ml HCl + 100 ml distilled water. The average grain size of each sample was determined using ImageJ software-based linear intercept method [6].

During the microstructural characterization, three images were acquired from each sample at identical magnifications and subsequently used for grain size determination. In total, 17 samples were analyzed. The standard deviation calculated for each specimen is presented, and is displayed as error bars in the corresponding figure.

Table 2. Sample codes based on annealing temperature and holding time

Sample code	Annealing temperature (°C)	Holding time (min)
A0	– (As-rolled)	– (As-rolled)
A1	150	10
A2	150	15
A3	150	20
A4	150	30
B1	200	10
B2	200	15
B3	200	20
B4	200	30
C1	250	10
C2	250	15
C3	250	20
C4	250	30
D1	300	10
D2	300	15
D3	300	20
D4	300	30

2.4. Nanoindentation hardness testing

According to ASTM E92-16, the thickness of the specimen should be at least ten times greater than the characteristic dimensions of the indenter to ensure reliable hardness measurements and minimize substrate effects [7]. In this study, since the copper foil had a final thickness of only 20 µm, conventional hardness testing methods could not be applied. Therefore, nanoindentation was employed as an appropriate technique to accurately measure the surface hardness of thin specimens.

Nanoindentation tests were performed using a TriboScope nanoindenter (manufactured by Hysitron, USA), equipped with a Berkovich diamond tip. For each annealing condition, three indentations were conducted. The average hardness value and the standard deviation for each sample were calculated. The selected applied load was 1000 µN to reflect true surface mechanical properties while minimizing substrate effects. The indentation depth varied depending on the hardness of each sample. The indent spacing was set to approximately 500 µm, as reported by the operator.

2.5. Electrical conductivity measurement

Due to the small thickness of the foils (20 µm), the four-point probe technique was chosen as the most accurate and reliable method for measuring electrical conductivity, while other methods, such as eddy current testing, were not suitable for thin samples [8].

Electrical conductivity measurements were performed utilizing the four-point probe (4PP) technique. Initially, the electrical resistance of the samples was measured. Subsequently, the electrical resistivity was calculated. The final electrical conductivity values were then reported in accordance with the International Annealed Copper Standard (%IACS) [9].

To assess the repeatability of the measurements, each sample was subjected to five replicate measurements.

The 4PP method, by effectively minimizing contact resistance, leads to a high degree of measurement accuracy. Consequently, the calculated standard deviation (SD) for the conductivity values was found to be remarkably small. For instance, for sample C1, the SD was determined to be 4.23×10^{-5} (%IACS). This negligible dispersion indicates that the associated uncertainty is below the graphical resolution for error bar representation on the resultant plot. A current of 10 mA was applied with a probe spacing of 20 mm. Equipment calibration was conducted using the electrical conductivity of fully annealed copper, standardized to 100% IACS.

3. Results and Discussion

3.1. Microstructural evolution

Representative optical microscopy images of selected samples are presented in Fig. 1. Sample A0 represents the copper foil that was cold rolled from an initial thickness of 100 µm down to 20 µm without any interpass annealing. As illustrated in the metallographic images, this condition is characterized by highly elongated and extensively deformed grains, with an average grain size of 17.64 µm. Considering the severe deformation and large thickness reduction applied during rolling, and the microstructural features observed, it is reasonable to infer that sample A0 retains a high degree of work hardening, substantial stored strain, and an elevated density of deformation-induced dislocations [10].

In the A-series samples (A1-A4), annealed at 150 °C, no significant microstructural changes were observed compared with the as-rolled state. The grain size gradually decreased from 16.78 µm (A1) to 15.02 µm (A4), but this reduction remained minor. However, a small drop in hardness (discussed in section 3.2) suggests that limited recovery may have occurred during these treatments [11].

In the B-series samples, annealed at 200 °C, a sharp decrease in grain size was observed, marking the onset of recrystallization. The average grain size decreased from 12.34 µm (B1) to 4.01 µm (B4), indicating extensive nucleation of strain-free recrystallized grains [12]. This refinement continued into the C-series, where the smallest grain size was recorded for sample C1 (3.47 µm), confirming that recrystallization was complete under this condition.

Beyond this stage, starting from C2 (4.41 µm), the grain size began to increase again, signaling the initiation of grain growth driven by the reduction of grain boundary energy [13]. Grain coarsening continued through the C-series and throughout the D-series, reaching 7.70 µm in sample D4.

Fig. 1 shows optical micrographs of representative samples (A0, A4, B4, C1, C4, and D4), illustrating the transition from elongated deformed grains to fine recrystallized structures and finally to coarser grains after extended annealing. The measured average grain sizes for all conditions are plotted in Fig. 2. Among all specimens, C1 exhibited the finest grain size (3.47 µm), while B4 (4.01 µm) also showed a significantly refined structure, indicating that these represent the optimum conditions from a microstructural perspective.

3.2. Nanoindentation hardness

The variation of nanoindentation hardness of all samples is presented in Fig. 3. The as-rolled sample (A0) exhibited the highest hardness value of 124.09 HV, which reflects the strong work hardening introduced during the cold rolling process [14].

No significant hardness drop was observed in the A-series samples (A1-A4). Although no significant change was detected in their microstructure, this slight softening (118.44 to 110.72 HV) suggests that a recovery process may have occurred, in which part of the stored deformation energy was reduced [15]. Such changes are not directly evidenced in this study but are consistent with the hardness reduction trend observed at these low annealing temperatures [16].

A more pronounced decrease in hardness was observed in the B-series and continued up to sample C1. This sharp reduction is attributed to the progressive occurrence of recrystallization, which replaced the heavily deformed structure with newly formed grains. The most significant hardness drop occurred at B1 (100.25 HV), indicating that recrystallization had started

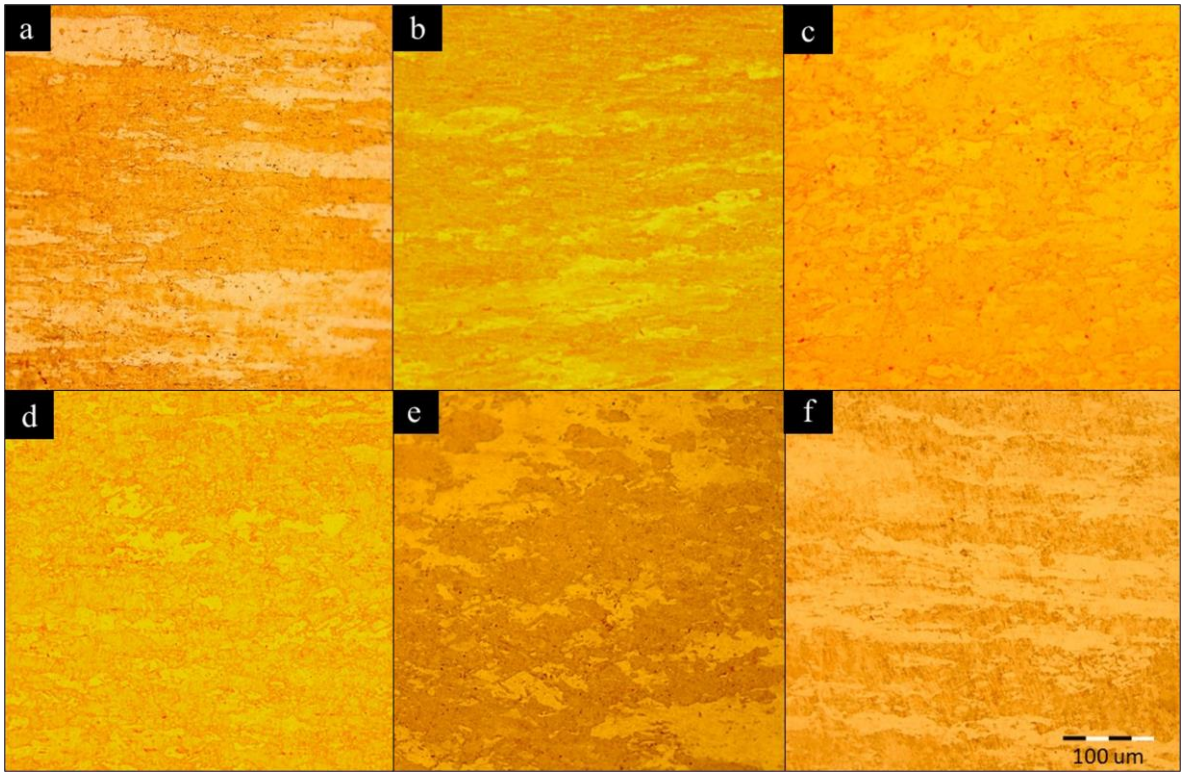

Fig. 1. Microstructures of selected samples: (a) A0, (b) A4, (c) B4, (d) C1, (e) C4, and (f) D4.

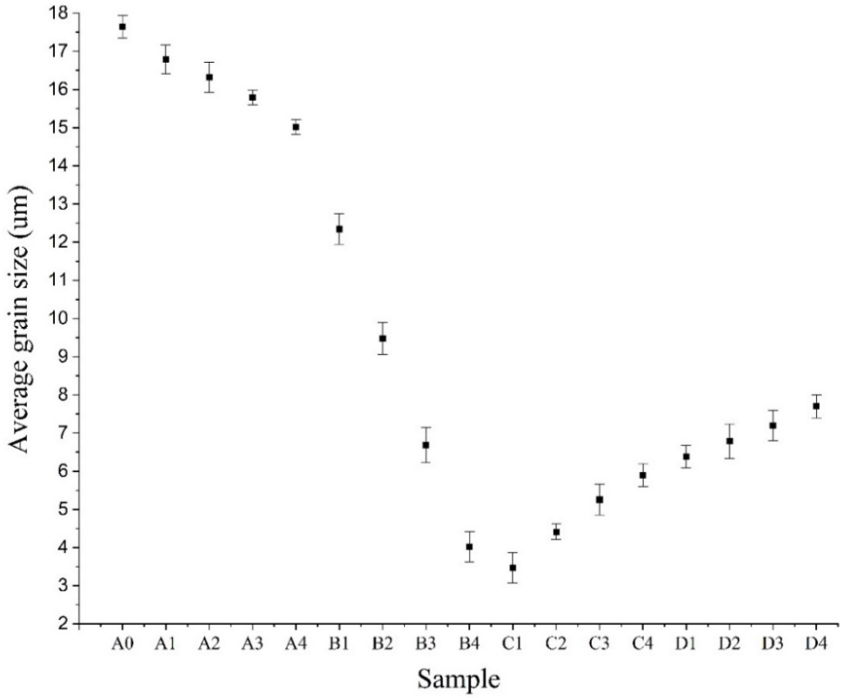

Fig. 2. Average grain size (μm) of each sample, calculated from surface optical micrographs.

under this condition and was completed by sample C1 (55.36 HV).

Beyond C1, as the annealing temperature and holding time further increased (C2-D4), the rate of hardness reduction diminished, and the hardness values became nearly constant within the D-series. This behavior is consistent with the expected grain growth stage, during which the overall microstructure coarsens,

but the hardness changes only slightly [17]. Among all conditions, sample D4 showed the lowest hardness of 44.67 HV, corresponding to the most extended annealing time and temperature.

In Fig. 4, the hardness variation as a function of annealing temperature is presented. The four curves correspond to annealing times of 10, 15, 20, and 30 minutes. As previously discussed, only minor changes in hardness were observed at 150 °C (A-series samples). In contrast, the most pronounced hardness reduction occurs at 200 °C and the initial part of 250 °C, which corresponds to the temperature range where recrystallization takes place.

Another critical factor influencing the time sensitivity observed at 200 °C is the surface-area-to-volume ratio (A/V) of the samples calculated as 5×10^4 m^{-1}. A high surface-area-to-volume ratio in the copper foil samples facilitates a rapid temperature equilibration throughout the entire sample. Consequently, the hardness of the annealed samples at 200 °C, situated within the recrystallization regime, exhibits heightened sensitivity to variations in annealing time.

While the rapid temperature equilibration due to a high surface-area-to-volume ratio is also applicable to other samples, its impact on time sensitivity differs. For instance, in samples annealed at 300 °C, the observed hardness variations are minimal within the grain growth regime, resulting in lower time sensitivity compared to the B-series samples.

As shown in Fig. 4, the lowest hardness gradient appears in the latter part of 250 °C and throughout 300 °C, where hardness changes are minimal. This behavior is directly associated with the grain growth stage of the annealing process [18].

3.3. Electrical conductivity

Since the copper foil in this study was designed for use in electronic applications, including printed circuit boards, lithium-ion batteries, and electromagnetic shielding, evaluating its electrical conductivity is essential for assessing functional performance [19]. The electrical conductivity of all samples, measured according to ASTM B667 and expressed in %IACS, is presented in Fig. 5.

According to the theory of electron transport in metals, structural defects, such as dislocation density, vacancies, and others, act as scattering centers that reduce electrical conductivity [20]. In this study, the as-rolled sample A0 exhibited the lowest conductivity, with a value of 84.39% IACS, which can be attributed to the

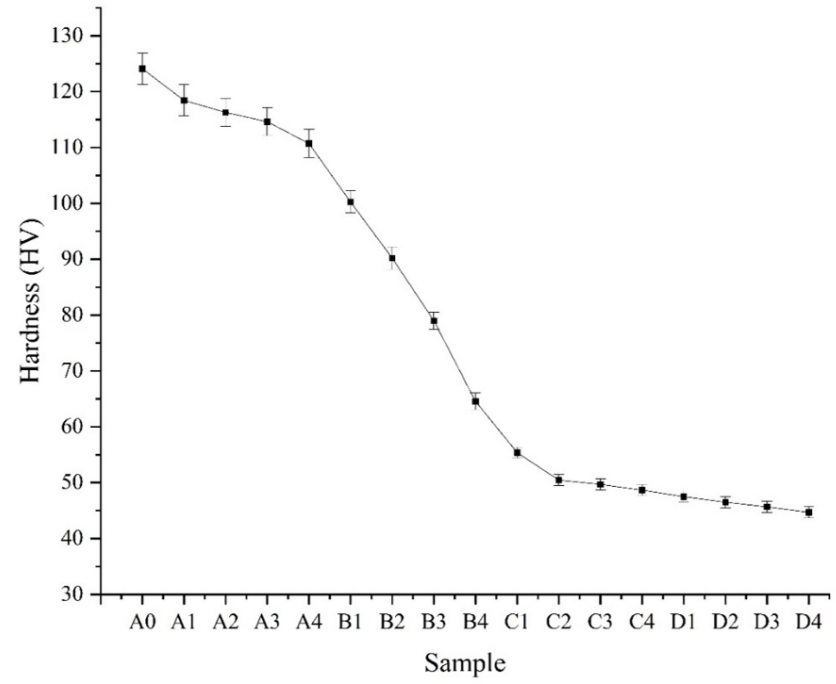

Fig. 3. Variation of nanoindentation hardness (Vickers) for each sample under different annealing conditions.

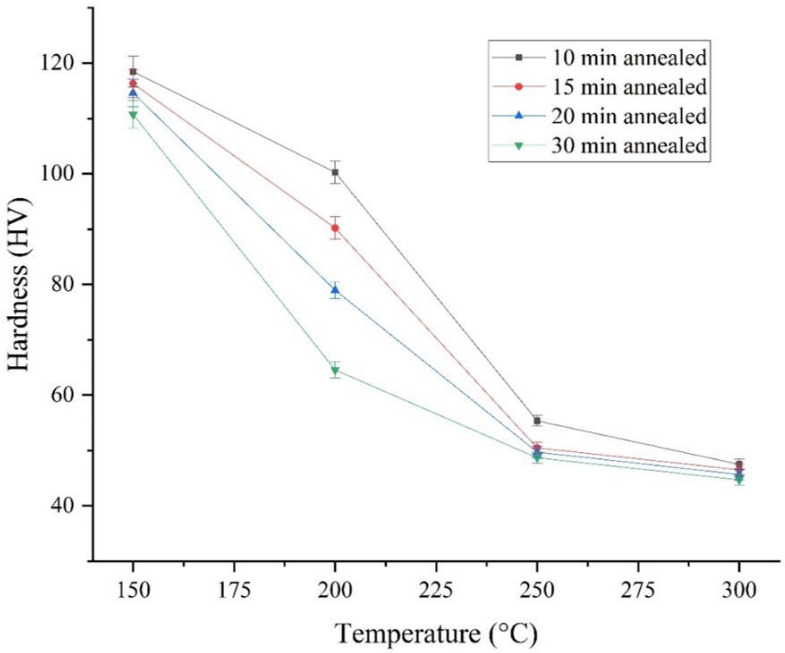

Fig. 4. Hardness variation of the copper foils as a function of annealing temperature for four annealing times (10, 15, 20, and 30 minutes).

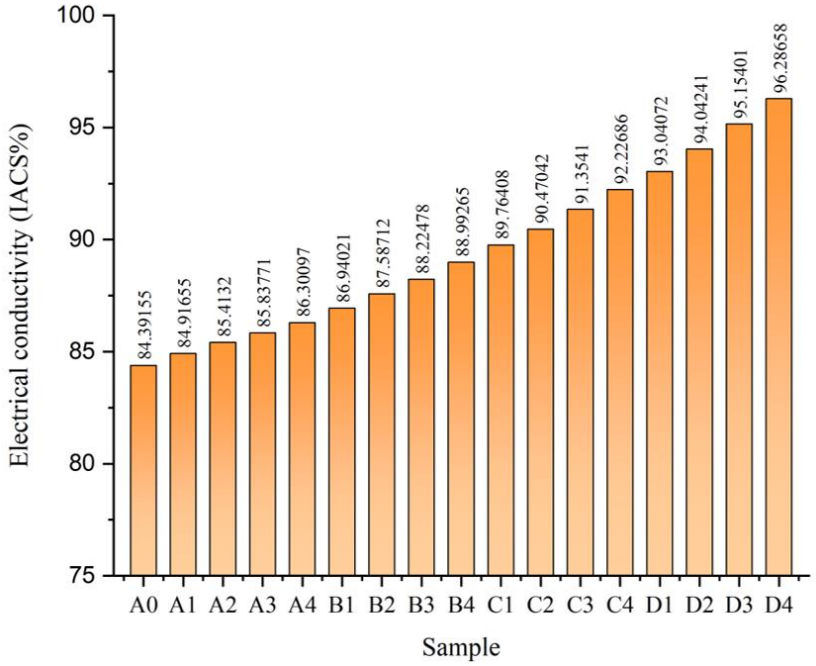

Fig. 5. Electrical conductivity (%IACS) of the copper foils as a function of annealing conditions for all samples (A0-D4).

large number of lattice defects introduced during severe plastic deformation [21].

Annealing treatment led to a gradual improvement in electrical conductivity. In the A-series samples (A1-A4), conductivity increased slightly from 84.92% IACS (A1) to 86.30% IACS (A4), is likely associated with partial recovery, during which a limited reduction of structural defects likely occurred [22].

In the B-series samples, a more pronounced increase in conductivity was observed, from 86.94% (B1) to 88.99% IACS (B4), which is consistent with the onset of recrystallization, where newly formed strain-free grains replace the highly deformed matrix. However, the nucleation of fine grains significantly increases the total

grain boundary area, and grain boundaries also act as electron-scattering barriers [23]. Two opposing effects coexist at this stage: reduction of lattice defects (increasing conductivity) and an increase in grain boundaries (reducing conductivity).

Microstructural observations confirmed the presence of the finest grains in the B-series and sample C1, which showed a conductivity of 89.76% IACS. The overall increase in conductivity in this region indicates that the reduction of lattice defects had a more dominant effect than the increase in grain boundary area [24].

Beyond C1, starting from C2 (90.47% IACS), recrystallization was completed, and most structural defects had been removed. The subsequent improvement in conductivity is therefore mainly attributed to grain growth, which reduces the total grain-boundary area [25]. This trend continued through the D-series, reaching its maximum in sample D4, which exhibited the highest conductivity at 96.29% IACS.

3.4. Correlation between grain size and hardness

The hardness and grain size of all samples are simultaneously shown in Fig. 6. Evaluating these two parameters together provides a clearer basis for identifying the optimum interpass annealing condition, while electrical conductivity must also be considered in the final selection. As illustrated in Fig. 6, the most desirable samples are those that exhibit the smallest grain size and relatively low hardness.

In thin copper foils, the grain size, and consequently the total grain-boundary area, has a direct and significant influence on the mechanical behavior of the foil cross-section [26]. Finer grains improve the mechanical properties of the foil cross-section [27].

The Hall-Petch relationship in the grain growth region (C1 to D4) was investigated [28]. According to Eq. (1), a plot of hardness versus inverse square root of grain size is illustrated in Fig. 7.

$$H = H_0 + k_h d^{(-1/2)} \quad (1)$$

As observed in Fig. 7, the behavior of the samples closely follows the linear Hall-Petch relationship. Through linear fitting, the slope and intercept were determined, yielding the equation presented in Eq. (2):

$$H = 31.92 + 49.04 d^{(-1/2)} \quad (2)$$

The slope of this fitted line, k_h = 49.03 HV.μm$^{1/2}$, indicates the influence of grain boundaries on the sample's hardness. It shows that as grain size increase, the hardness decreases significantly.

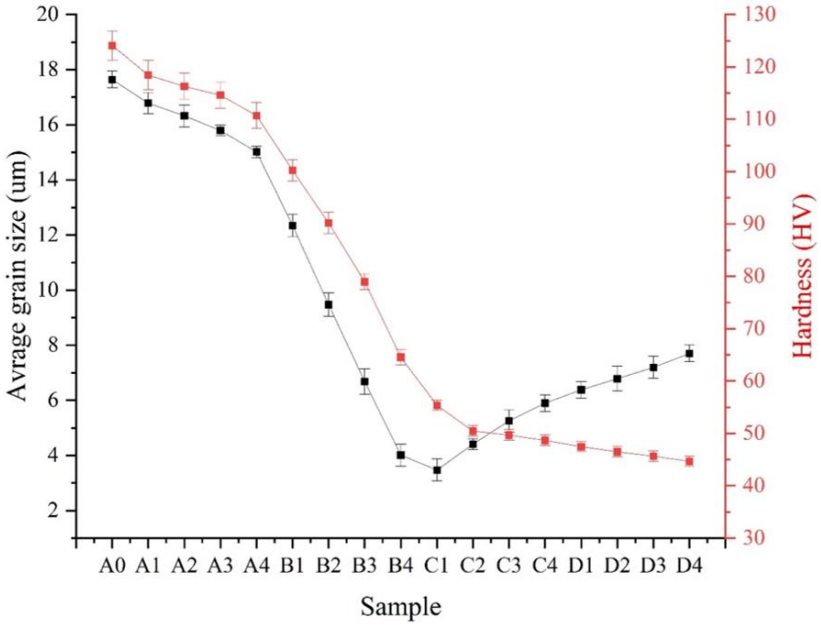

Fig. 6. Relationship between average grain size and nanoindentation hardness for all samples.

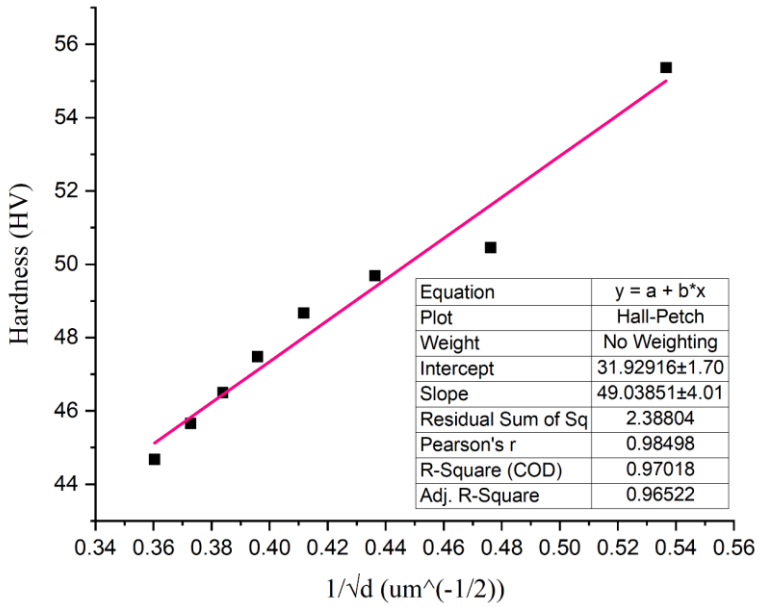

Fig. 7. Vickers hardness (HV) plotted as a function of the inverse square root of grain size ($d^{-1/2}$) for the grain growth region (e.g., C1-D4). The solid line represents the best-fit linear regression, which validates the Hall-Petch model.

The intercept (H_0 = 31.92 HV) denotes the intrinsic hardness of the base material in the absence of grain boundary effects, corresponding to a large or fully annealed grain structure [28]. This value is consistent with expectations, considering the material composition (TPC type copper).

Furthermore, the coefficient of determination, R^2 = 0.97, obtained from the linear fit, signifies a very strong agreement between the data and the Hall-Petch relationship, confirming the grain boundary strengthening behavior in this region.

4. Conclusion

According to the findings of this study, interpass annealing at 150 °C (A-series) did not yield favorable results. The A-series samples likely underwent only recovery, as indicated by the minor changes observed in grain size, hardness, and electrical conductivity. Therefore, annealing at 150 °C cannot be considered an effective condition for improving the properties of cold-rolled copper foils.

In contrast, annealing at 200 °C (B-series) produced significant improvements in microstructure and properties. Sample B4 (200 °C - 30 minutes) exhibited a refined grain structure with an average grain size of 4.01 µm, a reduced hardness of 64.56 HV, and an enhanced electrical conductivity of 88.99% IACS, indicating that this condition successfully promoted recrystallization and improves both mechanical and functional performance.

Similarly, sample C1 (250 °C - 10 minutes) demonstrated highly desirable characteristics, including an average grain size of 3.47 µm, a hardness of 55.36 HV, and a conductivity of 89.76% IACS. These properties indicate that short-duration annealing at 250 °C can achieve an excellent balance between grain refinement, mechanical softening, and electrical performance.

Although samples from C2 to D4 also exhibited adequate hardness and high electrical conductivity, their progressively increasing grain size was undesirable for producing thin 20 µm copper foils. Larger grains reduce the mechanical stability of the foil cross-section [29].

Furthermore, higher annealing temperatures and longer holding times are not practical for industrial production, as they increase energy consumption, extend processing time, and impose additional operational costs. Extended annealing also accelerates surface oxidation, which is detrimental to foil quality and can severely damage surface integrity.

Overall, the results indicated that the most effective interpass annealing conditions are represented by B4 (200 °C - 30 minutes) and C1 (250 °C - 10 minutes). Depending on equipment capabilities and production requirements, either of these two conditions can be selected as the optimal route for manufacturing high-quality copper foils suitable for electronic applications.

Authors' contributions

A. A. Shahbazi: Investigation, Data curation, Methodology, Writing original draft, Writing - review & editing

H. R. Shahverdi: Conceptualization, Methodology, Supervision

A. A. Mottahedi: Methodology, Supervision

Conflict of interest

The authors declare that they have no known competing financial interests or personal relationships that could influenced the work reported in this paper.

Funding

The authors thank the Department of Materials Engineering of Tarbiat Modares University (TMU) for financial support of this study.

Data availability

The data that support the findings of this study are available upon request from the corresponding author.

5. References

[1] Davis, J. R. (2001). *Copper and copper alloys*. ASM International.

[2] Sousa, T. G. D., Sordi, V. L., & Brandão, L. P. (2017). Dislocation density and texture in copper deformed by cold rolling and ECAP. *Materials Research*, *21*(1), e20170515. https://doi.org/10.1590/1980-5373-mr-2017-0515

[3] Chen, J., Xu, W., Yang, J., Yang, Z., Shi, H., Lin, G., Li, Z., Shen, X., Jiang, B., Liu, H., & Gui, K. (2024). Effects of cold rolling path on recrystallization behavior and mechanical properties of pure copper during annealing. *Transactions of Nonferrous Metals Society of China*, *34*(10), 3233-3250. https://doi.org/10.1016/S1003-6326(24)66605-7

[4] Wang, L., Bai, Z., Sun, W., Du, L., Peng, X., Xiao, Y., Zhang, J., Jia, Y., Du, S., Cai, H., & Liu, E. (2023). Effect of low temperature annealing on microstructure and properties of copper foil. *Materials Today Communications*, *36*, 106617. https://doi.org/10.1016/j.mtcomm.2023.106617

[5] Shi, H., Gan, W., Esling, C., Zhang, Y., Wang, X., Maawad, E., Stark, A., Li, X., & Wang, L. (2023). Recrystallization texture evolution of cold-rolled Cu foils governed by microstructural and sample geometrical factors during heating. *Materials Characterization*, *196*, 112605. https://doi.org/10.1016/j.matchar.2022.112605

[6] E04 Committee. (2013). *Test methods for determining average grain size*. ASTM International. https://doi.org/10.1520/E0112-13

[7] E28 Committee. (2003). *Test method for Vickers hardness of metallic materials*. ASTM International. https://doi.org/10.1520/E0092-16

[8] E1004-23 Committee. (2017). *Test method for determining electrical conductivity using the electromagnetic (eddy-current) method*. ASTM International. https://doi.org/10.1520/E1004-17

[9] ASTM B667 - 97 Committee. (2019). *Practice for construction and use of a probe for measuring electrical contact resistance*. ASTM International. https://doi.org/10.1520/B0667-97R19

[10] Hosford, W. F., & Caddell, R. M. (2007). *Metal Forming*. Cambridge University Press. https://doi.org/10.1017/CBO9780511811111

[11] Clemens, H., Mayer, S., & Scheu, C. (2017). Microstructure and properties of engineering materials. *Neutrons and Synchrotron Radiation in Engineering Materials Science*, 1-20. Wiley. https://doi.org/10.1002/9783527684489.ch1

[12] Humphreys, F. J., & Hatherly, M. (2012). *Recrystallization and related annealing phenomena*. Elsevier. https://doi.org/10.1016/B978-0-08-044164-1.X5000-2

[13] Cao, J., Zhang, J., Tang, H., Shen, X., Song, K., Zhou, Y., & Cui, C. (2025). Investigation on the microstructure evolution and strengthening behavior of rolled bonding Cu strip. *Journal of Science: Advanced Materials and Devices*, *10*(1), 100835. https://doi.org/10.1016/j.jsamd.2024.100835

[14] Merchant, H. D., Liu, W. C., Giannuzzi, L. A., & Morris, J. G. (2004). Grain structure of thin electrodeposited and rolled copper foils. *Materials Characterization*, *53*(5), 335-360. https://doi.org/10.1016/j.matchar.2004.07.013

[15] Bhaduri, A. (2018). *Mechanical Properties and Working*

of Metals and Alloys, 264. Springer Singapore. https://doi.org/10.1007/978-981-10-7209-3

[16] Hosford, W. F. (2005). *Mechanical Behavior of Materials*. Cambridge University Press. https://doi.org/10.1017/CBO9780511810930

[17] Feng, R., Zhao, W., Sun, Y., Wang, X., Gong, B., Chang, B., & Feng, T. (2022). Softened microstructure and properties of 12 μm thick rolled copper foil. *Materials*, *15*(6), 2249. https://doi.org/10.3390/ma15062249

[18] Song, M., Liu, X., & Liu, L. (2017). Size effect on mechanical properties and texture of pure copper foil by cold rolling. *Materials*, *10*(5), 538. https://doi.org/10.3390/ma10050538

[19] Chen, Z., Fu, H., Zhang, C., Chen, J., Xu, Y., Zheng, Y., Zhong, Y., Wang, X., Gu, C., & Tu, J. (2025). Copper foils for high-energy-density lithium batteries: Composite vs. ultrathin. *Journal of Energy Storage*, *139*, 118917. https://doi.org/10.1016/j.est.2025.118917

[20] Ziman, J. M. (2007). *Electrons and phonons: The theory of transport phenomena in solids*. Clarendon Press; Oxford University Press.

[21] Mayadas, A. F., & Shatzkes, M. (1970). Electrical-resistivity model for polycrystalline films: The case of arbitrary reflection at external surfaces. *Physical Review B*, *1*(4), 1382-1389. https://doi.org/10.1103/PhysRevB.1.1382

[22] Solouki, H., Jamaati, R., & Aval, H. J. (2025). Influence of asymmetric rolling paths on the microstructure, texture, mechanical behavior, and electrical conductivity of electrolytic tough pitch copper. *Materials Chemistry and Physics*, *332*, 130246. https://doi.org/10.1016/j.matchemphys.2024.130246

[23] Bishara, H., Lee, S., Brink, T., Ghidelli, M., & Dehm, G. (2021). Understanding grain boundary electrical resistivity in Cu: The effect of boundary structure. *ACS Nano*, *15*(10), 16607-16615. https://doi.org/10.1021/acsnano.1c06367

[24] Xiong, S., Sun, J., Xu, Y., & Yan, X. (2015). Effect of lubricants and annealing treatment on the electrical conductivity and microstructure of rolled copper foil. *Journal of Electronic Materials*, *44*(7), 2432-2439. https://doi.org/10.1007/s11664-015-3772-y

[25] Solouki, H., Jamaati, R., & Jamshidi Aval, H. (2024). High-temperature annealing behavior of cold-rolled electrolytic tough pitch copper. *Heliyon*, *10*(12), e33276. https://doi.org/10.1016/j.heliyon.2024.e33276

[26] Shingledecker, J., Griscom, E., & Bridges, A. (2023). Relationship between grain size and sample thickness on the creep-rupture performance of thin metallic sheets of INCONEL alloy 740H. *Journal of Materials Engineering and Performance*, *32*(20), 9309-9322. https://doi.org/10.1007/s11665-022-07785-2

[27] Souza, C. R. D., & Monlevade, E. F. D. (2021). Effect of cold rolling path on the deformation textures of C10300 copper. *Materials Research*, *24*(2), e20200332. https://doi.org/10.1590/1980-5373-mr-2020-0332

[28] Chang, S. Y., & Chang, T. K. (2007). Grain size effect on nanomechanical properties and deformation behavior of copper under nanoindentation test. *Journal of Applied Physics*, *101*(3). https://doi.org/10.1063/1.2432873

[29] Zhang, H. M., Dong, X. H., Wang, Q., & Peng, F. (2013). The experimental and numerical investigation on the mechanical properties of metallic foil. *Advanced Materials Research*, *705*, 228-233. https://doi.org/10.4028/www.scientific.net/AMR.705.228